Liquid Crystals
Publication details, including instructions for authors and subscription information:
http://www.informaworld.com/smpp/title~content=t713926090

On the phase sequence of antiferroelectric liquid crystals and its relation to orientational and translational order

Jan P. F. Lagerwall[a]; Per Rudquist[a]; Sven T. Lagerwall[a]; Frank Gießelmann[b]
[a] Dept. of Microelectronics & Nanoscience, Chalmers University of Technology, SE-412 96 Göteborg, Sweden, [b] Institute of Physical Chemistry, Clausthal University of Technology, D-38678 Clausthal-Zellerfeld, Germany,

To cite this Article Lagerwall, Jan P. F. , Rudquist, Per , Lagerwall, Sven T. and Gießelmann, Frank(2003) 'On the phase sequence of antiferroelectric liquid crystals and its relation to orientational and translational order', Liquid Crystals, 30: 4, 399 — 414
To link to this Article: DOI: 10.1080/0267829031000069683
URL: http://dx.doi.org/10.1080/0267829031000069683

Liquid Crystals, 2003, Vol. 30, No. 4, 399–414

Taylor & Francis
Taylor & Francis Group

On the phase sequence of antiferroelectric liquid crystals and its relation to orientational and translational order

JAN P. F. LAGERWALL*, PER RUDQUIST, SVEN T. LAGERWALL
Dept. of Microelectronics & Nanoscience, Chalmers University of Technology,
SE-412 96 Göteborg, Sweden

and FRANK GIEßELMANN
Institute of Physical Chemistry, Clausthal University of Technology,
D-38678 Clausthal-Zellerfeld, Germany

(*Received 7 June 2002; in final form 21 October 2002; accepted 5 November 2002*)

The substance MHPOBC is the oldest and still most important reference antiferroelectric liquid crystal (AFLC). There is still considerable controversy concerning the correct phase designations for this material and, in particular, about the presence or absence of SmC* in its phase sequence. By means of dielectric spectroscopy and polarizing microscopy, we show that whereas the pure compound lacks the SmC* phase, this phase rapidly replaces the SmC$_\beta^*$ subphase through the reduced purity resulting from temperature-induced chemical degradation which is hard to avoid under standard experimental conditions. X-ray investigations furthermore show that this change in phase sequence is coupled to a decrease in translational order. This explains the large variations in the reported phase sequence and electro-optic behaviour of MHPOBC, in particular concerning the SmC$_\beta^*$ phase which has been said to exhibit ferro-, ferri- as well as antiferroelectric properties. It is likely that the sensitivity of the AFLC phase sequence to sample purity is a general property of AFLC materials. We discuss the importance of optical and chemical purity as well as tilt and spontaneous polarization for the observed phase sequence and propose that one of the key features determining the existence of the different tilted structures is the antagonism between orientational (nematic) and translational (smectic) order. The decreased smectic order (increased layer interdigitation) imposed by chemical impurities promotes the synclinic SmC* phase at the cost of the AFLC phases SmC$_\alpha^*$, SmC$_\beta^*$, SmC$_\gamma^*$ and SmC$_a^*$. We also propose that the SmA* phase in FLC and AFLC materials may actually have a somewhat different character and, depending on its microstructure, some of the tilted phases can be expected to appear or not to appear in the phase sequence. AFLC materials exhibiting a direct SmA*–SmC$_a^*$ transition are found to be typical 'de Vries smectics', with very high orientational disorder in the SmA* phase. Finally, we discuss the fact that SmC$_\beta^*$ and SmC$_\gamma^*$ have two superposed helical superstructures and explain the observation that the handedness of the large scale helix may very well change sign, while the handedness on the unit cell level is preserved.

1. Introduction

At an early stage in the study of antiferroelectric liquid crystals (AFLCs) it was recognized that these materials may exhibit not only the antiferroelectric SmC$_a^*$ phase, but also three other so-called *subphases*, the characteristics of which proved to be much more difficult to establish. In the pioneering studies of MHPOBC (4-(1-methylheptyloxycarbonyl)phenyl 4′-octyloxybiphenyl-4-carboxylate, cf. the table) which still today is the prototype AFLC compound, the phases emerging on cooling from the isotropic phase were designated SmA*–SmC$_\alpha^*$–SmC$_\beta^*$–SmC$_\gamma^*$–SmC$_A^*$ [1]. (In this work we write the latter phase SmC$_a^*$.) Experiments soon showed that the subphases, SmC$_\alpha^*$, SmC$_\beta^*$ and SmC$_\gamma^*$, disappear from the phase diagram in favour of the ordinary, synclinic SmC* phase, on decreasing the optical purity [1, 2], i.e. on adding larger and larger amounts of the enantiomer with opposite handedness. In the racemate, only SmC$_a$ and SmC prevail.

The middle subphase, SmC$_\beta^*$, has lately received much attention. It was long thought to be equivalent to the ordinary SmC* phase [2, 3], but later studies on samples

---

*Author for correspondence; e-mail: jan_lagerwall@mac.com

Liquid Crystals ISSN 0267-8292 print/ISSN 1366-5855 online © 2003 Taylor & Francis Ltd
http://www.tandf.co.uk/journals
DOI: 10.1080/0267829031000069683

Table. Chemical constitutions and phase sequences (temperatures in °C) of the compounds discussed. The phase sequence of (*S*)-MHPOBC is based on the results of the dielectric spectroscopy measurements on the fresh sample in this work.

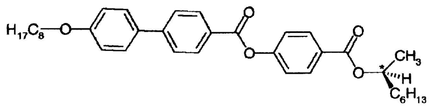 (*S*)-MHPOBC	$\mathrm{Crystal} \underset{59}{\longleftarrow} (\mathrm{SmI}_{a}^{*}) \underset{67}{\overset{84}{\rightleftarrows}} \mathrm{SmC}_{a}^{*} \underset{118.5}{\overset{119.5}{\rightleftarrows}} \mathrm{SmC}_{\gamma}^{*} \underset{119.7}{\overset{120.5}{\rightleftarrows}} \mathrm{SmC}_{\beta}^{*} \underset{121.2}{\overset{121.9}{\rightleftarrows}}$ $\mathrm{SmC}_{\alpha}^{*} \underset{122.5}{\overset{123.0}{\rightleftarrows}} \mathrm{SmA}^{*} \underset{149.5}{\overset{150.2}{\rightleftarrows}} \mathrm{Isotropic}$
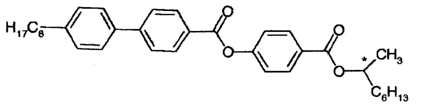 MHPBC	Crystal–60–SmC_{a}^{*}–65–$\mathrm{SmC}_{\gamma}^{*}$–68–$\mathrm{SmC}_{\beta}^{*}$–72–$\mathrm{SmC}_{\alpha}^{*}$–76–SmA*–109–Isotropic (From [39].)
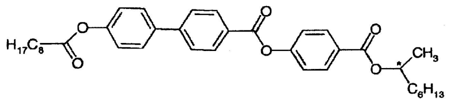 MHPOCBC	Crystal–(73)–(SmI_{a}^{*})–77.9–SmC_{a}^{*}–100.5–$\mathrm{SmC}_{\alpha}^{*}$–106.5–SmA*–148.1–Isotropic (From [40].)
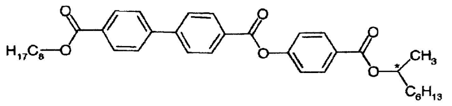 MHPOOCBC	Crystal–40.0–$\mathrm{SmC}_{\gamma}^{*}$–41.9–SmC*–87.2–SmA* (From [21]. Note that in a graphic in the same paper, the temperature range of $\mathrm{SmC}_{\gamma}^{*}$ is instead reported to be 43°C–52°C.)
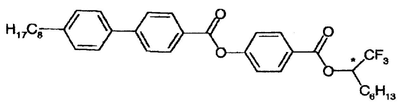 TFMHPBC	SmC_{a}^{*}–74.3–$\mathrm{SmC}_{\alpha}^{*}$–75.0–SmA* (From [20].)
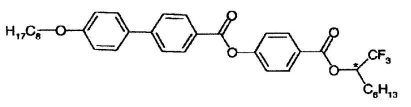 TFMHPOBC	Crystal–75–SmX*–86–SmC_{a}^{*}–111–SmA*–124–Isotropic (From [41]. The phase transition temperatures are given with very low accuracy. The phase denoted SmX* is probably SmI_{a}^{*}.)
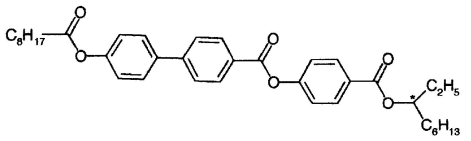 EHPOCBC	Crystal–66.9–SmC_{a}^{*}–93.3–SmA* (From [21].)
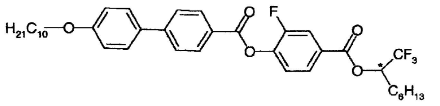 10BIMF6	Crystal–30–SmC_{a}^{*}–75.9–SmA*–95.0–Isotropic (From [24].)

of high optical purity have shown that this conclusion was premature. Several investigators have attributed ferrielectric properties to the phase [4–7]. Recently, Gorecka and co-workers [8] reproduced the early racemization experiments on MHPOBC, starting out with an (*S*)-enantiomer sample of exceptional purity, and showed that SmC_{β}^{*} is neither ferrielectric nor equal to ordinary SmC*. Their experimental results instead showed that it is identical to the *antiferroelectric* subphase which has been identified in several other AFLC compounds [9, 10]; in the following we will therefore use the notation SmC_{β}^{*} for this subphase (which was given the name 'AF' by the Fukuda group when they first clearly identified the phase in the compound

MHPBC [9]). The frequent observation of the SmC* phase, and the absence of the antiferroelectric subphase, in the phase sequence of MHPOBC can be interpreted as an effect of imperfect sample purity. Likewise, the impression that SmC^*_β exhibits 'ferrielectric' properties can be understood as a consequence of phase coexistence between the antiferroelectric SmC^*_β and the ferroelectric SmC* [11] in samples that were nearly, but not completely, pure.

In the last few years our knowledge of the SmC^*_β and SmC^*_γ phases has improved considerably, largely due to resonant X-ray and ellipsometry experiments carried out at Brookhaven and in Minnesota, respectively [12–15]. There now seems to be a general consensus that the basic repeating unit (often referred to as unit cell) in both cases is biaxial and that its size is four layers in SmC^*_β and three layers in SmC^*_γ. The exact structure of the repeating unit is still not clear, but the most probable description seems to be some kind of highly distorted clock structure—the directors of the different layers in the unit cell are not co-planar, but the biaxiality shows that they can also not be symmetrically distributed around the layer normal [14, 16].

In the present work, starting with a sample of (*S*)-MHPOBC pure enough to exhibit the SmA*–SmC^*_α–SmC^*_β–SmC^*_γ–$\mathrm{SmC}^*_\mathrm{a}$ phase sequence, we show by means of dielectric spectroscopy combined with texture monitoring, that the SmC* phase develops at the cost of SmC^*_β, not only on doping with the opposite enantiomer, but also if the sample is just kept at temperatures in the range ~90°C – ~125°C, i.e. where the different versions of the chiral smectic C phase family are stable. The varying behaviour reported for MHPOBC may thus be related not only to differences in optical or chemical purity of the initial compound, but also to continuous sample degradation induced by the experimental investigation of the subphases in this compound. Jakli [6] also noticed continuously decreasing phase transition temperatures during a long term experiment on MHPOBC, but he reported no further changes in the phase sequence.

We have also carried out corresponding long term X-ray diffraction studies, and noted that the diffraction pattern observed within the temperature range of the chiral smectic C family of phases changes characteristics drastically as a result of sample aging, indicating that the thermally induced degradation is chemical decomposition. Such a process can be expected to result in a decrease in smectic order (increase in layer interdigitation); in the discussion we develop a simple reasoning illustrating how this decreased order may well be the reason for the disappearance of the subphases on reducing the purity of antiferroelectric liquid crystal materials in general. Hence, the discussion will concern not only MHPOBC but we will also use examples from several other AFLC materials. We pay particular attention also to the differences in orientational order between FLCs and AFLCs and to the influence of tilt and spontaneous polarization on the different chiral smectic C type phases.

Several notation schemes have been proposed for the AFLC subphases. In this paper we use the original notation of the Fukuda school, i.e. the three subphases are denoted SmC^*_α, SmC^*_β and SmC^*_γ. Towards the end of the paper we will justify this choice and discuss how the rather chaotic AFLC terminology situation can be improved.

2. Experimental

Dielectric spectroscopy studies were performed using an HP 4192 dielectric bridge (5 Hz to 13 MHz measuring range), on cooling and on heating. The measuring field amplitude was 10 mV μm^{-1} and no d.c. bias was applied during the experiments. The liquid crystal was filled by capillary action in the isotropic phase into home-made planar-aligning cells with a substrate spacing of 23 μm. These were equipped with ITO electrodes and rubbed polyimide as alignment layer (antiparallel rubbing). When a uniformly aligned, defect free sample was desired, this was achieved by applying an 80 Hz square wave, with an amplitude above the threshold for switching into the synclinic state of the $\mathrm{SmC}^*_\mathrm{a}$ phase, on cooling from the isotropic liquid. When the $\mathrm{SmC}^*_\mathrm{a}$ phase had been reached, the frequency was reduced to 20 Hz and the amplitude was then slowly decreased to zero. The sample was kept in a custom-made liquid-heated hot stage, the temperature of which was controlled by a Julabo FP-25HD circulator. The actual sample temperature was monitored with a PT100 sensor inserted into the sample holder. The hot stage was mounted in a Leitz polarizing microscope (crossed polarizers) by means of which the sample texture was monitored throughout the course of the dielectric measurements, using a Sony video camera connected to the measurement computer via a National Instruments framegrabber card. All MHPOBC textures in this paper were photographed with the polarizer cross turned 3° away from the extinction position of the sample in the SmA* phase.

For the X-ray measurements, performed on unaligned (powder-like) samples, the liquid crystal was filled into Mark glass capillary tubes of 0.7 mm diameter. Small angle scattering data were obtained using a CuK_α radiation source, a Kratky-compact camera (A. Paar) and a one-dimensional electronic detector (M. Braun), giving a measure of the layer spacing with a resolution better than 0.1 Å in the range of interest. The sample was mounted in a brass block, the temperature of which was controlled using an A. Paar temperature controller.

3. Results

3.1. *Dielectric spectroscopy and textural observations*

3.1.1. *The fresh sample*

The dielectric response and selected textures, representative of the different chiral smectic C type phases, in a fresh sample are shown in figure 1. From the dielectric absorption spectra (*a*) and (*j*) it is easy to identify the different smectic phases. At high temperatures, the SmA* phase (light grey in the spectra) is distinguished by the characteristic soft mode. Its increasing susceptibility and decreasing critical frequency on cooling towards the SmC$_{\alpha}^{*}$ phase announce the onset of collective polar order in the latter phase. Within the SmC$_{\alpha}^{*}$ phase (green) a single mode, with approximately the same susceptibility and frequency as the soft mode at the transition, is active. The SmC$_{\beta}^{*}$ phase (red), following after SmC$_{\alpha}^{*}$ on cooling, is distinguished by an almost complete absence of dielectric absorption (apart from the spurious cell relaxation due to the finite resistance of the ITO electrodes), reflecting the antiferroelectric order of this phase. From its weak response it may easily be distinguished from the next subphase, SmC$_{\gamma}^{*}$ (light blue), which exhibits the strongest polar mode among the phases of the fresh MHPOBC sample. Its large susceptibility—reflecting a non-zero mesoscopic polarization—and low critical frequency indicate that the response is due to collective fluctuations in the phase angle, e.g. a distortion of the SmC$_{\gamma}^{*}$ helix. At the transition to the antipolar, antiferroelectric SmC$_{a}^{*}$ phase (dark blue), finally, the response is again very weak and the strongest absorption seen in the spectrum is the cell relaxation.

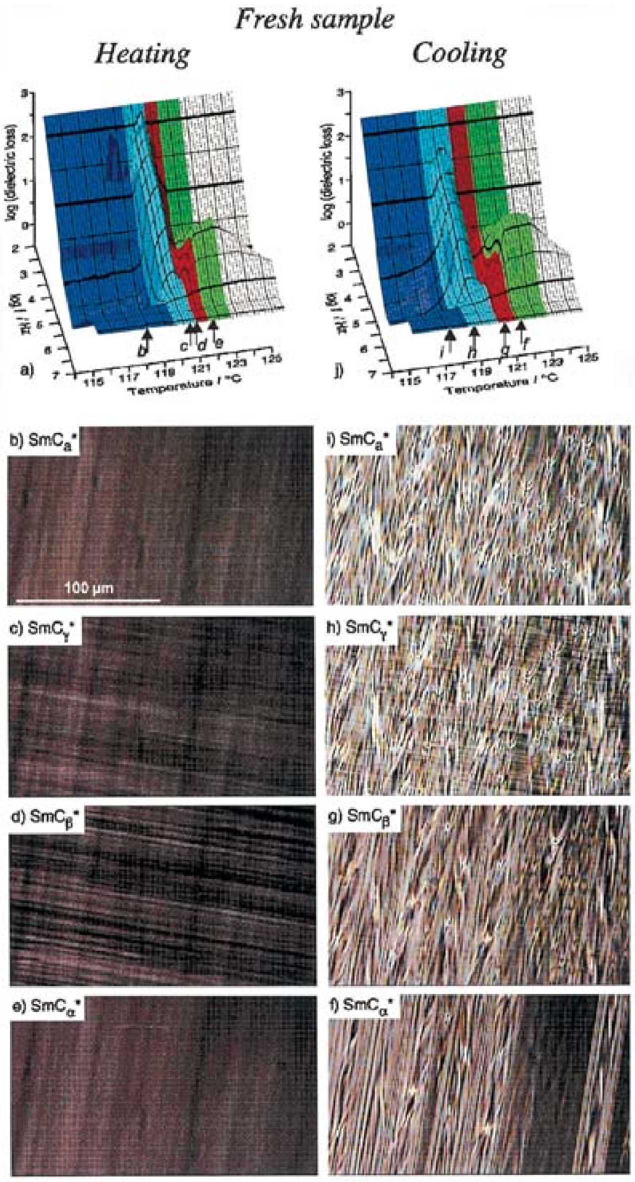

Figure 1. Dielectric loss spectra (*a* and *j*) and selected textures obtained on a fresh sample of (*S*)-MHPOBC on heating (left column) and subsequent cooling (right column). The texture examples on heating are: (*b*) SmC$_{a}^{*}$ (118.0°C), (*c*) SmC$_{\gamma}^{*}$ (120.4°C), (*d*) SmC$_{\beta}^{*}$ (120.8°C), (*e*) SmC$_{\alpha}^{*}$ (121.7°C). On cooling from the SmA* phase, the corresponding textures are: (*f*) SmC$_{\alpha}^{*}$ (121.2°C), (*g*) SmC$_{\beta}^{*}$ (120.3°C), (*h*) SmC$_{\gamma}^{*}$ (118.6°C) and (*i*) SmC$_{a}^{*}$ (117.2°C). The smectic layer normal runs approximately in the one o'clock direction.

Before the first measurement, which was performed on heating from SmC$_{a}^{*}$, the sample was uniformly aligned. Except for the helix unwinding lines, the images (*b*) to (*e*) in figure 1 therefore show essentially uniform textures of SmC$_{a}^{*}$, SmC$_{\gamma}^{*}$, SmC$_{\beta}^{*}$ and SmC$_{\alpha}^{*}$, respectively. The SmC$_{a}^{*}$ and SmC$_{\alpha}^{*}$ textures are, apart from the minor change in birefringence colour, almost identical, but the SmC$_{\gamma}^{*}$ and SmC$_{\beta}^{*}$ phases are distinguished by distinct lines parallel to the smectic layers, reflecting the rather long helical pitch of these phases. The contrast of these helix unwinding lines varied with temperature within both these phases, but the periodicity was always in the order of a few microns.

The first cooling measurement followed directly upon the heating run, with the turning point a few degrees into the SmA* phase. As is clear from textures (*f*) to (*i*), a large number of defects now spontaneously formed within the tilted phases. At the SmA*–SmC$_{\alpha}^{*}$ transition, the uniform, dark SmA* texture was divided into two types of ribbon directed along the buffing direction of the sample cell. In one type, the layer direction of the SmA* phase was seemingly intact (these ribbons had in principle the same dark colour as in SmA*); in the other the layers folded in a horizontal chevron structure, giving rise to bright, 'fishskin-like' defects. We have observed this division into two structures earlier for other AFLC materials [17], and then deduced that the horizontal chevron structure arose from the alternating directions of the helix unwinding lines, either in the long pitch subphases or in the SmC* phase under application of an electric field of intermediate strength, producing a partially unwound helical structure. The folding of the layers into horizontal or vertical chevrons is a result of shrinking layer thickness, giving rise to dilative strain in the smectic.

In thick samples, as in our case, there is a tendency for the chevron structure to relax into the closely related low energy structure of parabolic confocal domains [18]. Such parabolic domains are hardly observed in thin samples, as they require a certain depth both in the horizontal and vertical plane in order to form. The transition to SmC$_\beta^*$ was easily recognized in the texture by a sudden appearance of a large number of small parabolic focal-conic defects; on further cooling, these merged into large parabolic defects. The helix unwinding lines were also visible, but with much poorer contrast than in the uniform texture seen in the preceding heating experiment. On cooling back into the SmC$_a^*$ phase, finally the helix unwinding lines disappeared, but the parabolic focal-conics remained.

3.1.2. *Degradation of the sample—the emergence of the SmC* phase*

After the first two measurements, the sample was kept at 90°C for four days. Thereafter, one set of heating and cooling runs was carried out every day. In between measurements, the sample was kept at 90°C or, after day thirteen, at 100°C. As illustrated in the diagrams in figure 2, all phase transition temperatures continuously decreased during this time. A much more drastic change took place after thirteen days, possibly connected with the slightly increased stand-by temperature (the exact choice of stand-by temperature should have no qualitative influence on the process, but the higher temperature naturally speeds up degradation). During the cooling measurement there was now clear evidence, both in the textures and in the dielectric spectrum (figure 3) for SmC* in the phase sequence. Judging from the spectrum, the SmC* phase (yellow) seems to have replaced the SmC$_\beta^*$ phase, as the typical SmC* helix distortion mode, with a susceptibility one order of magnitude larger than that of the strongest mode of the fresh sample, is now seen between the SmC$_\alpha^*$ and SmC$_\gamma^*$ phases. Thus our sample now exhibited the phase sequence which has most often, though incorrectly, been quoted for optically and chemically pure MHPOBC. Based on the dielectric spectrum alone, it is impossible to say if there are also remnants of the SmC$_\beta^*$ phase coexisting with SmC*, since the response of the SmC$_\beta^*$ phase is so weak; any SmC$_\beta^*$ response will be completely overwhelmed by the strong SmC* helix distortion mode.

The emergence of the SmC* phase also had a large impact on the texture sequence. Down to the low temperature end of the SmC$_\alpha^*$ phase, the texture appeared as in the equivalent situations earlier in the study. However, below the transition, the texture was completely different from the corresponding texture of the earlier runs, figure 3 (*d*), reflecting that the phase below SmC$_\alpha^*$ was no longer SmC$_\beta^*$, but rather SmC*. Several of the bright, fishskin-like defects and many parabolic focal-conics had disappeared, leaving a more ordered, mainly black texture, decorated with fewer defect flashes and few, well separated, low contrast helix unwinding lines along the layers. On cooling through SmC*, the lines grew in number and contrast and the periodicity became better defined, stabilizing at about 2.5 μm. If a sample of MHPOBC exhibiting a SmC* phase is prepared such that the layers form parallel to the sample plane (the SmA* phase is homeotropically aligned), it generally shows visible selective reflection in the temperature range of this phase, illustrating that the SmC* helical pitch is rather short. The very coarse lines seen in the SmC* phase of the 13 days old sample reflect a much larger pitch, and it thus seems likely that the new SmC* phase indeed coexists with the old SmC$_\beta^*$ phase.

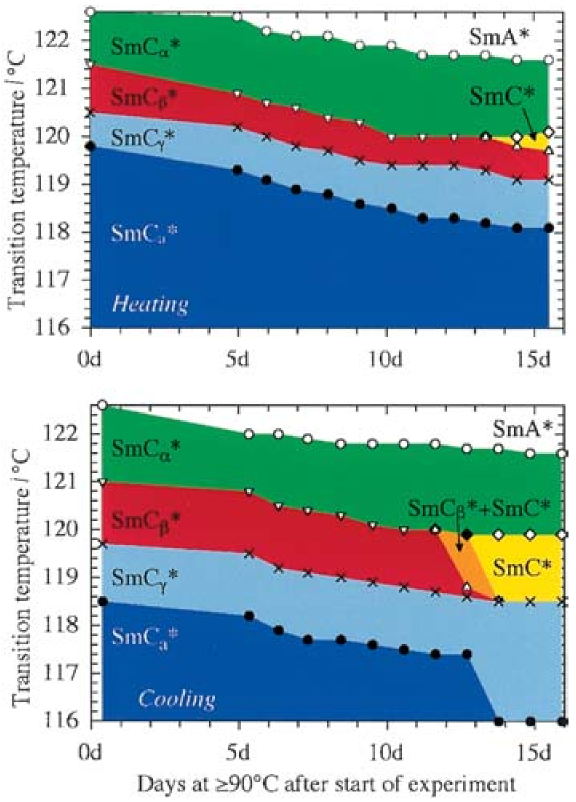

Figure 2. Phase sequence on heating (upper) and on cooling (lower) as a function of time.

At the transition to SmC$_\gamma^*$, the texture was again dramatically changed, figure 3 (*e*). Broad white ‘streets’ appeared along the layers and the remaining fishskin-ribbons were broken up into smaller branches. During

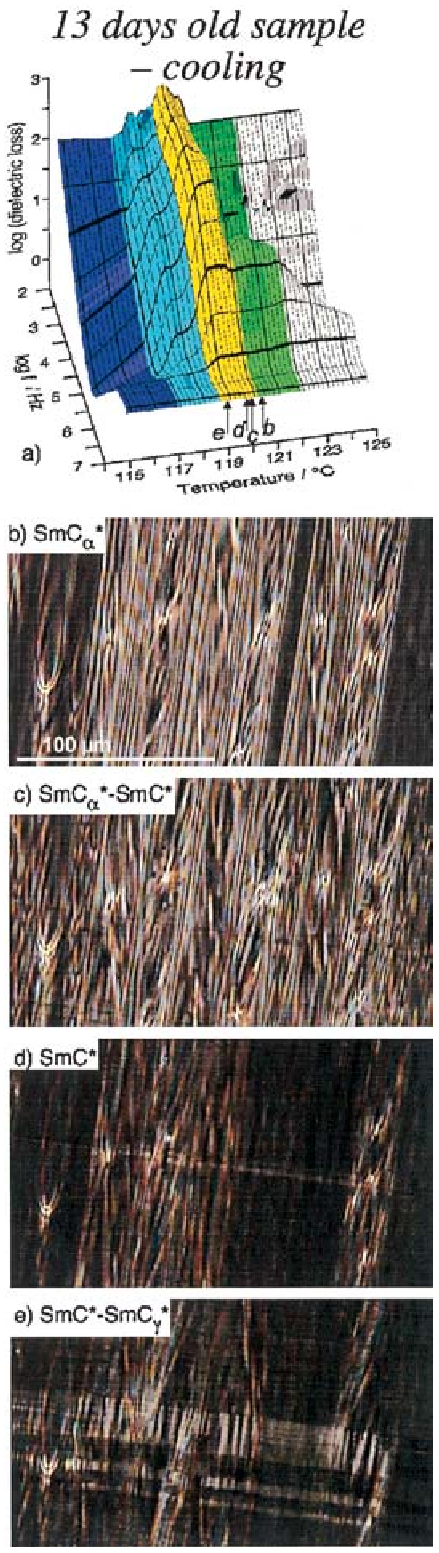

Figure 3. Dielectric loss spectrum (*a*) and selected textures obtained on the 13 days old sample on cooling. This was the first run where the SmC* phase appeared. The texture examples are: (*b*) SmC$_\alpha^*$ (120.3°C), (*c*) the SmC$_\alpha^*$–SmC* transition (119.9°C), (*d*) SmC* (119.7°C) and (*e*) the SmC*–SmC$_\gamma^*$ transition (118.9°C).

the transition these branches moved laterally and also changed direction slightly. On further cooling, the white layer-parallel ribbons slowly separated into helix unwinding lines and at the same time a large number of new parabolic focal-conics appeared.

The violent texture changes on both sides of the SmC* phase are *a priori* difficult to explain, but they indicate that SmC* exhibits a structure clearly different from the other MHPOBC phase structures. While there was a large degree of paramorphosis in the texture sequence SmC$_\alpha^*$ to SmC$_a^*$ before the emergence of the SmC* phase, there is no resemblance whatsoever between the textures below and above the SmC* phase once this has entered the phase sequence. All this, together with the fact that the fresh sample exhibits no SmC* phase at all, are in fact strong indications that the synclinic, synpolar SmC* phase has the character of an alien phase in the AFLC phase sequence, appearing only as a result of sample decomposition of one kind or another. We will return to this matter in § 4.

In heating experiments, the phase sequence without SmC* persisted slightly longer, but when the sample was 15 days old the SmC* phase was unmistakably present, as easily seen in the dielectric spectrum, see figure 4 (*a*). In contrast to the cooling runs, however, the SmC$_\beta^*$ phase could still be observed on its own in a small temperature window between SmC$_\gamma^*$ and SmC*. In the textures of figures 4 (*b*–*d*), the appearance of the SmC* phase was not as dramatic as on cooling. The paramorphotic features were more evident and there was also a notable decrease in the number and/or visibility of the defects in the SmC* texture, distinctly darker than the much hazier SmC$_\beta^*$ and SmC$_\alpha^*$ textures. Both transitions, SmC$_\beta^*$–SmC* and SmC*–SmC$_\alpha^*$, are clearly first order as evidenced by the coexistence easily seen in figures 4 (*c*) and 4 (*d*): the new phase entered as thin, sharp lines along the layers. On further heating these continuously grew in width until they covered the whole image. The coexistence of the two phases in both cases lasted several minutes and over a temperature span of ~0.3°C.

In our very first investigations of the pure MHPOBC batch, prior to the long term experiment described here, the SmC* phase appeared much earlier. The reason for the longer time period before the emergence of the SmC* phase during the systematic experiment may be the fairly gentle treatment of the sample. Most of the time the sample was kept at 90°C, and no high voltages were ever applied. During the earlier investigations, which were carried out much more as liquid crystals are usually studied, high a.c. or d.c. switching voltages were often applied and the sample was kept in the subphase temperature range (~120°C) most of the time. We can thus conclude that the degradation of a sample of MHPOBC

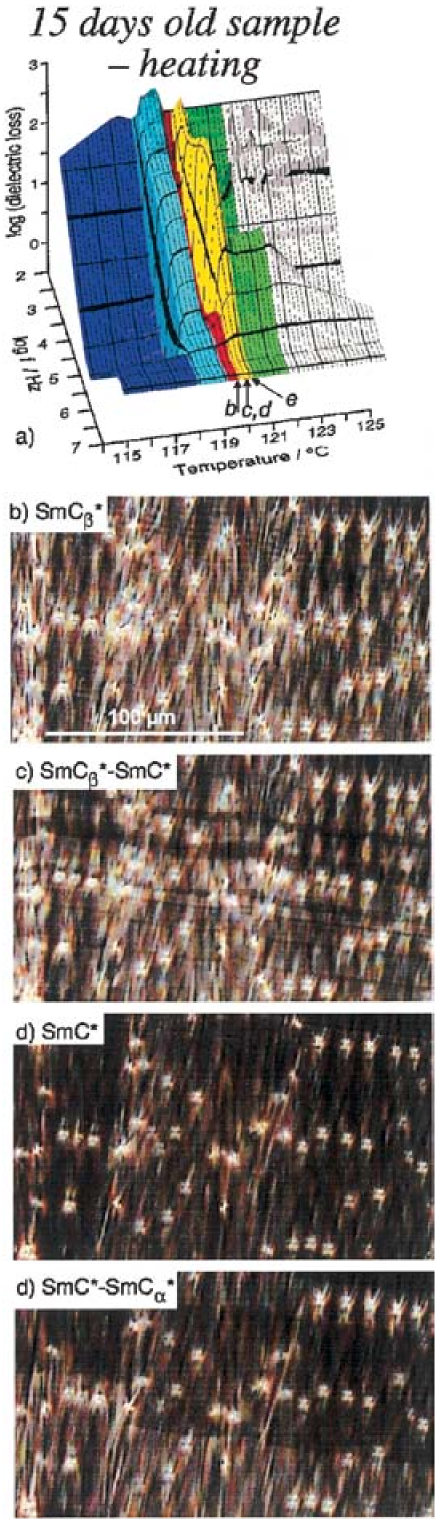

Figure 4. Dielectric loss spectrum (*a*) and selected textures obtained on the 15 days old sample on heating. This was the first heating run where the SmC* phase was detected. The texture examples are: (*b*) SmC$^*_\beta$ (119.5°C), (*c*) the SmC$^*_\beta$–SmC* transition (119.9°C), (*d*) stable SmC* (119.9°C, somewhat later) and (*e*) the SmC*–SmC$^*_\alpha$ transition (120.1°C).

may take place much faster during normal investigations involving, for instance, electro-optic techniques.

We should finally consider the possibility that the change in phase behaviour could be induced by contamination from the aligning layers, rather than degradation of the liquid crystal itself. There are several indications that this is not the prime reason, if it at all plays a role. First, the type of sample cells used for the present studies have been successfully employed for many other compounds without observing similar changes in phase sequence. Second, the many different reports regarding the MHPOBC phase sequence also support the idea that this molecule is easily degraded. Finally, the X-ray investigations, to be described below, were performed using glass capillary tubes without any alignment layers. Here also, drastic changes were observed after some time at high temperatures.

3.2. *X-ray investigations*

In order to obtain a different and independent view of the degradation process we performed small angle X-ray scattering investigations in a long term experiment similar to the dielectric spectroscopy/texture monitoring experiment. The primary aim was to investigate whether the layer spacing changed as the sample was degraded, but it turned out that the entire scattering properties of the sample shifted rather dramatically. Measurements were in general made on heating from SmC$^*_a$ to SmA* and then on cooling back to SmC$^*_a$. Only during the first measurement, carried out on cooling the sample from the isotropic phase, was the cooling run done first. Between measurements, the sample was kept at approximately 100°C, protected from the X-ray radiation. Unfortunately, the $\sim \pm 1$ K temperature control accuracy did not allow for a detailed investigation of the most interesting temperature region (just below the onset of tilt). However, the results still give much information on a general level about the sample degradation process.

Figure 5 shows the X-ray scattering profiles as a function of temperature, on heating and on cooling, at three different occasions during the experiment. All diagrams have the same scale. The fresh sample (upper row) exhibited fairly clean single scattering peaks in all smectic phases, and the typical behaviour of the layer spacing, reaching a global maximum in the SmA* phase just above the transition to the tilted phases, was easily recognized (see also figure 6). Relative to the scattering intensity in the SmA* phase formed on initial cooling from the isotropic phase, we observed an increase in intensity on cooling through the different smectic C type phases. The intensity saturated at a level in the SmC$^*_a$ phase which was fairly stable during the whole reheating measurement. This change indicates that the translational (smectic) order along the layer normal increased on

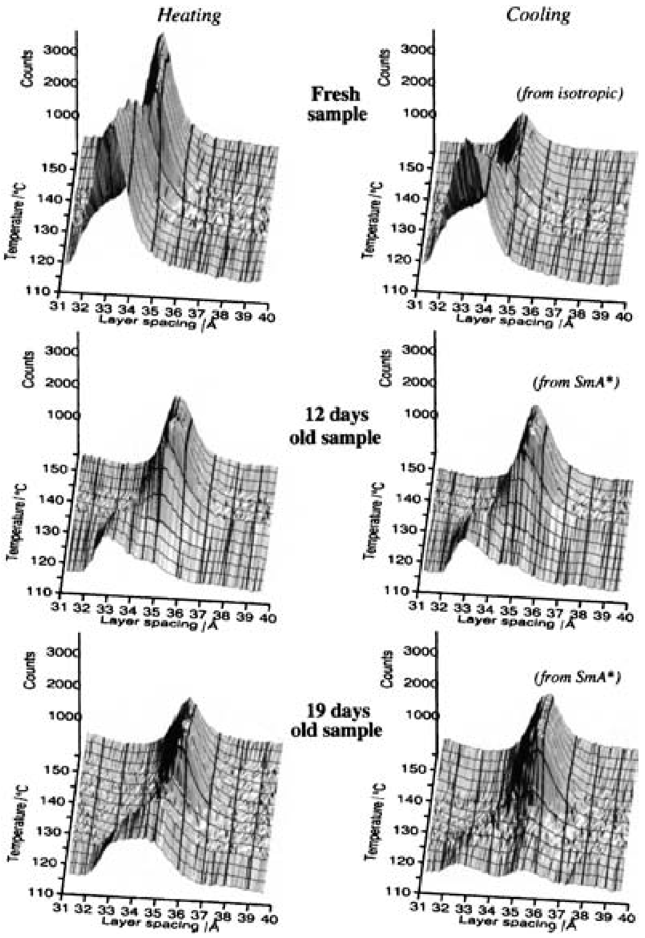

Figure 5. The process of sample degradation as seen through X-ray diffraction. For further comments, see the main text.

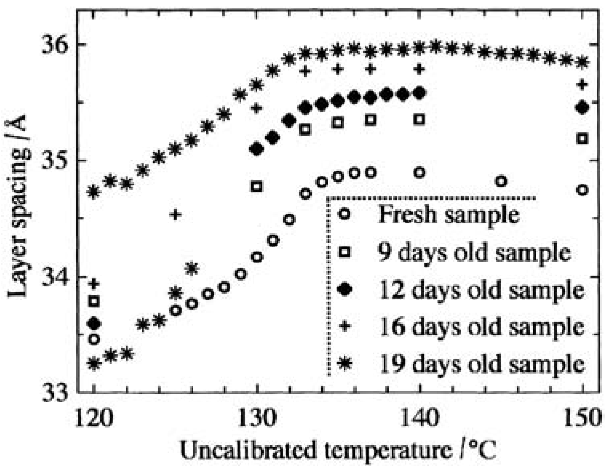

Figure 6. The effect of sample degradation on the smectic layer spacing, as obtained through X-ray scattering, measured on heating. In the 19 days old sample, two values of layer spacing coexist at low temperatures.

cooling into the tilted smectic phases. During re-heating, the intensity of the first order peak visible in figure 5 was essentially constant, reflecting that the smectic order was less affected by heating the sample, provided that the clearing point was not reached.

The scattering profile of the twelve days old sample (middle row) differs from the virgin sample response in several ways. The centre of the SmA* scattering peak has moved to the right, reflecting an increase in layer spacing. Furthermore, the SmA* scattering intensity, which was approximately the same as that during the first heating measurement, is now much larger than in the tilted phases. The lower scattering intensity observed in the smectic C type phases indicates that the smectic order parameter now *decreased* on entering the tilted phases. A possible explanation for this can be found in the third, most conspicuous, change: a splitting of the scattering peak of the tilted phases. This splitting became more and more obvious during the continuing experiment. The splitting into two incommensurate scattering peaks indicates that the sample simultaneously exhibits two different periodicities below the onset of tilt. In other words, it seems that the thermal degradation actually induces a coexistence of phases with different layer spacing below the SmA* phase. It is not difficult to imagine that such a situation affects the translational order adversely.

The separation into two phases is easily conceivable in bulk volumes with no aligning surfaces, as in the capillaries used for the X-ray scattering experiments. The situation is quite different in the 23 μm thick sample used for dielectric and texture investigations. In addition to the smallest dimension there being almost two orders of magnitude smaller, the surfaces are also coated with alignment layers imposing a strong unidirectional planar, and possibly strongly polar, anchoring. Under such restrictions it may be more likely that the one of the two phases most favoured by the environmental conditions, or even yet another phase, completely dominates. Hence, we cannot directly correlate the observed phase changes discussed in § 3.1 with the changes in X-ray scattering profile. However, the processes giving rise to the changes in the dielectric spectra and X-ray data are likely to be the same in both cases.

An important general observation is that the peak splitting was not as evident in the heating measurements as on cooling, related to the fact that the heating measurements were carried out after a stand-by time at ~100°C of approximately 20 h. This indicates that the structure with two coexisting phases, appearing at the transition from SmA* into the tilted phases, was metastable. During the stand-by time until the following heating experiment, the system could relax towards a more stable state. Its scattering profile, where the two peaks from the cooling experiment have almost merged into one broad peak, indicates that the system was now mainly characterized by a single structure with a periodicity roughly between those of the two phases first formed on cooling.

The layer spacing varied slightly throughout the experiment. As the absolute numbers depend on a proper calibration of the equipment, which may not be valid after a time period of several days, one must interpret these results with some care. However, on a general level it seems that the layer spacing increases as the sample degrades, as illustrated in the diagram in figure 6, showing data obtained during heating measurements.

4. Discussion

After more than ten years of intense research, the question of the origin of syn- and anti-clinic order in smectics still remains unresolved. The three subphases constitute an even more complex problem. We will here try to relate our experimental observations to what is known from the literature and to discuss the matter of clinicity and the appearance and disappearance of subphases in terms of smectic and nematic order, as well as magnitude of the tilt and the electric polarization. The observation of chemical degradation of the MHPOBC sample after several days at elevated temperatures is perhaps not surprising, although the fact that a laboratory study of the chiral smectic C type phases always takes the sample to these temperatures, hence induces the degradation, has not been pointed out earlier. This degradation leads to the introduction of the synclinic SmC* phase at the cost of the subphases. Below we will try to give an explanation of this behaviour.

As a determination of the exact nature of the contaminants appearing in the aged MHPOBC sample is an extensive research project in itself, such an analysis is not included in the present work. In this paper we are more concerned about the general effects of introducing foreign molecules into an AFLC compound, in particular how the decrease in order induced by the presence of contaminants can be expected to have a large impact on the phase sequence. For this discussion the particular chemical nature of the contaminants is not of prime importance, and so we postpone the chemical analysis to a future paper.

4.1. *The importance of optical and chemical purity*

The well known high sensitivity of antiferroelectric liquid crystal phases to optical purity [1, 2], in particular the vanishing of subphases with only a minor decrease in enantiomeric excess, would perhaps suggest that a change in some kind of chiral interaction would be responsible for the appearance or disappearance of the different subphases. The Ljubljana school has developed a phenomenological model, in line with this approach, in which different phase structures arise as the values of parameters representing chiral interactions are varied [8, 19]. However, the reduction in optical purity necessary to expel the subphases is very small (of the order of a few percent) and it is not obvious why this would dramatically affect the strengths of the chiral interactions. Even if chirality is required—in the sense that it is responsible for polarity and polar interactions in these materials—for the formation of the subphases, one must also consider the possibility that a change in certain parameters not related to chirality, for instance the degree of translational (smectic) order, may drastically influence the effect of chiral as well as polar interactions, and thereby destabilize certain phases and promote others. As an illustration, let us consider the SmA*–N* transition. Obviously, the chiral strength, or helical twisting power, does not increase drastically on heating into the N* phase. It is just as high in SmA*, but as the layered structure of this phase is incompatible with a helical director modulation, there is (disregarding the TGB case) no macroscopic structural evidence of the chirality. We propose that the sensitivity to sample purity of the antiferroelectric subphases is likewise not related primarily to changes in chiral interactions, but rather to changes in smectic order.

The direct correlation between chirality and the AFLC phase sequence also runs into problems when considering that there are several cases of AFLC compounds which do not exhibit subphases, even in their optically purest (as yet synthesized and reported) state. In fact, Isozaki *et al.* even observed that TFMHPBC (see the table), which in its optically pure state exhibits a SmA*–SmC$^*_\alpha$–SmC$^*_a$ phase sequence, developed the other two subphases, SmC$^*_\gamma$ and SmC$^*_\beta$, when the optical purity was *lowered* to 80% e.e [20]. It is also difficult to discuss the variation in the strength of chiral interactions when mixing two different optically pure chiral compounds. For instance, the above Japanese group observed that the antiferroelectric SmC$^*_\beta$ subphase develops between a 40% and 80% mixing ratio when mixing MHPOOCBC and MHPOCBC (see the table) [21]. If this observation is correct, and the emergence of SmC$^*_\beta$ were linked to ‘increased chirality’, the mixture should be ‘maximally chiral’ between a mixing ratio of 40% and 80%. We find such an explanation problematic and therefore suggest carrying out the analysis in different terms.

Moreover, the subphases generally vanish when we mix an AFLC compound exhibiting the subphases with a compound (FLC or AFLC) where these phases are not present, and this takes place for any choice of stereospecific enantiomers. Hence the phenomenon of subphase suppression can plausibly be assumed to be a general feature of mixing sufficiently different molecules, thereby influencing steric and polar interactions, but not necessarily their chiral aspects. Also the case of controlled reduction in optical purity by doping a pure compound with its opposite enantiomer can be understood in these terms, as the optimum packing of opposite enantiomers may be quite different from the case where only one enantiomer is present. Mixtures where the subphases are not destabilized (or, in rare cases, even enhanced) are always, to our knowledge, binary mixtures, the components of which are both AFLCs exhibiting the subphases. In general they are also structurally very similar to one another, e.g. MHPOCBC and MHPOOCBC [21].

The stabilization of less ordered phases by mixing different components is a quite general phenomenon. As is well known, liquid crystals used in displays or in similar applications always consist of multi-component mixtures in order to sufficiently increase their practical temperature range. Such a mixture has to preserve its thermodynamic phase and be prevented from crystallization. This is achieved by mixing different compounds, resulting in an increase of entropy in the liquid crystalline phase and thus a decrease in the crystallization temperature. We can also understand the process by considering that there is no lattice available into which the mixture could crystallize if the components are sufficiently dissimilar. Hence, a phase separation has to take place prior to leaving the liquid crystalline state for a crystalline one. In such a case we are dealing with crystallization and order in three dimensions. The corresponding phenomenon in lower dimensionality is far more subtle. In the case of smectics, and in particular in the family of chiral smectic C phases, we are dealing with different forms of crystallization in one dimension. As correlations fall off rapidly in low-dimensional systems we have every reason to expect that, in addition to incommensurate helical structures, only a few kinds of commensurate structure may exist in smectic systems. As we add a foreign material to an optically pure AFLC compound we diminish more and more the distance over which correlations can be fully effective across layers. We would therefore expect the subphase with longest unit cell to vanish first. Thus SmC_β^* and SmC_γ^* should disappear in that order, which is also what we find experimentally. Finally, only the normal two-layer unit cell $\mathrm{SmC}_\mathrm{a}^*$ phase can exist in addition to the SmC* phase. Having the smallest possible unit cell, it is always the SmC* phase that becomes more and more stable as the sample purity is reduced.

4.2. *The importance of translational order*

As one of the first recognized major problems in employing AFLCs in display devices was the difficulty in obtaining a uniform alignment, a prime goal for materials development research has been to find AFLCs exhibiting a chiral nematic phase (much easier to align than SmA*) at temperatures above the antiferroelectric $\mathrm{SmC}_\mathrm{a}^*$ phase. But this proved to be a very difficult task and, still today, not one antiferroelectric liquid crystal material has been found which also exhibits a cholesteric phase. In a rare case [22] where a compound has been reported to have both a N* phase and a $\mathrm{SmC}_\mathrm{a}^*$ phase, we believe that this is an incorrect assignation of the latter, solely based on the observed electro-optic behaviour. Most probably, what in that case is interpreted as the tri-state electro-optic response of a $\mathrm{SmC}_\mathrm{a}^*$ phase is a field-induced first order SmA*–SmC* transition, one which has the same field-symmetry properties as the tri-state switching in $\mathrm{SmC}_\mathrm{a}^*$ and which can easily be mistaken as such.

The lack of N* in the phase sequence of AFLCs is an indication that the tendency to form layers in these materials is much stronger than in FLCs, in which there is often a cholesteric phase above the SmA* phase. The anticlinic structure of $\mathrm{SmC}_\mathrm{a}^*$ and the orientational order without translational order in the nematic phase represent extreme examples on the smectic order–disorder scale in liquid crystals, and it is unlikely to find both phases in the same compound. If a nematic phase will ever be observed in an antiferroelectric liquid crystal material it could only be expected as a result of very smart mixing. We may thus in antiferroelectric liquid crystals expect higher smectic order parameter values, i.e. sharper boundaries between layers with less molecular interdigitation. It is not difficult to find support for this in published experimental work. Als-Nielsen *et al.* performed X-ray scattering experiments on the achiral single liquid crystal compound CBOOA, exhibiting a nematic phase above SmA, and concluded that the molecular interdigitation across the layer interfaces in the SmA phase in this case can reach the point of giving the electron density variation along the smectic layer normal an almost sinusoidal character [23]. If a tilted phase develops under such circumstances, it is obvious that tilting in the same direction in adjacent layers, i.e. synclinic order, must be strongly promoted. As pointed out by Takanishi *et al.* [24], such a low degree of translational order is actually more or less incompatible with an anticlinic, antiferroelectric structure: a large number of the molecules of the sample will find themselves in the diffuse boundaries between two layers where, in the case of an overall anticlinic structure, the tilt direction would be undefined. The Japanese group also carried out X-ray experiments, comparing the first, second and third order layer diffraction peaks as a function of temperature in racemic MHPOBC and in an optically pure sample of the AFLC compound 10BIMF6. They noticed that the intensity of all peaks, but in particular of the higher order ones, increased markedly below the transition to the anticlinic phase, showing that the smectic order parameter is indeed rather high in the AFLC phases. We also note that in the interpretation of an IR experiment by Jin *et al.* [25], the chiral end chain in MHPOBC is reported to make a large average angle to the core axis, rendering the average molecular shape considerably more bent. This would reduce interdigitation and increase the smectic order parameter.

We should point out that a large smectic order does not mean that steric interactions across the layer boundaries are absent. On the contrary, these may actually be important in the stabilization of anticlinic structures. It has been postulated that the origin of anticlinic order in non-chiral swallow-tail liquid crystals exhibiting the SmC_a phase, are the steric interactions across the layer boundaries between the branched ends of the molecular tails [26, 27]. The important issue in our discussion is the degree of localization of the centres of mass of the molecules to a single layer—if this is weak, as expressed by a (quasi)sinusoidal electron density distribution along the layer normal, the formation of anticlinic structures is disfavoured.

It is also important to note that steric interactions are by definition short range. In principle one can imagine different kinds of layer interface (adjacent directors synclinic, anticlinic, or out-of-plane) being promoted by steric interactions, as illustrated by the swallow-tail example, but they promote the interface to be the same for *all* layer boundaries. Therefore, strong steric interactions should have the effect of destabilizing any structure with a unit cell of more than two layers where the layer interfaces are *not* all equal, as in the proposed distorted clock structures for the SmC^*_β and SmC^*_γ phases. Hence, such structures can be allowed only in the case of a relatively low degree of interdigitation.

The X-ray results in the present study suggest that the aged MHPOBC sample is no longer a single compound, but a mixture consisting of MHPOBC together with products of chemical decomposition of this molecule. For simplicity, let us assume that the molecules decompose at one specific bond. We would then expect molecules of at least three different lengths: the original MHPOBC length, and the lengths of the two separated components. Once the degree of decomposition reaches a certain level, the only way of achieving a high packing efficiency under the restriction of well defined smectic layers (i.e. high smectic order), must be to separate molecules of different lengths. Hence, we may expect small islands of shorter molecules, presumably still forming a layered structure, within the MHPOBC matrix. But the X-ray results indicate that such a separation occurs only at temperatures below the SmA* phase. The tilted smectic structures obviously have larger difficulty in incorporating molecules of different length in a single phase. We believe that this is a result of the required increase in translational order connected with the tilting transition.

4.3. *AFLCs and the de Vries description of smectic order*

Another order-related issue which may have large relevance to the understanding of AFLCs is the important, but today often overlooked, recognition of de Vries that the imperfect orientational order of all liquid crystals has a big impact on the smectic microstructure and its description [28–30]. In all smectic phases, including SmA (and SmA*), there must actually be a non-zero average molecular inclination with respect to the layer normal; if all molecules were aligned along the layer normal, this would imply a nematic order parameter of $S=1$, but a typical value in smectics is $S \sim 0.8$, corresponding to an average tilt of about 20°. The uniaxial properties, in particular the director being along the layer normal, of the SmA (SmA*) phase show that all tilting directions are equally probable. The molecular long axes can thus be thought of as uniformly distributed on a diffuse cone, the axis of which coincides with the director and layer normal in the SmA* phase.

If a macroscopic director tilt arises, as in a smectic C type phase or in the SmA* phase under application of an electric field (electroclinic effect), this can be interpreted in two ways. Either the cone axis (i.e. the centre of orientational fluctuations) has started to tilt away from the layer normal, or the degeneracy in tilt directions has been broken, such that one particular direction of tilt is now energetically favoured. Most certainly, both processes occur together, but the relative importance varies between different materials. At least there must always be a certain degree of azimuthal biasing present since, for any non-zero director tilt, the cone surface will suffer a polar as well as a quadrupolar deformation. On the other hand, if the orientational order is very low, corresponding to a large average molecular inclination and thus a wide diffuse cone, the biasing process could in principle explain the whole optical tilt on its own. This would result in the very attractive property of a smectic layer thickness which is completely unaffected by the onset of tilt; but such materials are very rare. Almost all smectics show some shrinkage of the layer spacing connected with increasing director tilt θ (even though less than the magnitude of θ would suggest) [31].

One can perform a simple experimental test to investigate the balance between the processes responsible for the appearance of the macroscopic tilt. In a material which in the SmA* phase exhibits a wide de Vries cone, the appearance of a non-zero optical tilt angle can be expected to be mainly related to a biasing of the tilting directions. This reduces the orientational disorder, and hence increases the effective birefringence Δn [32]. Therefore, such a material should not only exhibit a large electroclinic effect in the SmA* phase (with a high field saturated tilt roughly corresponding to the angle at the cone surface), but the effect would, in particular, be connected with a change from low to high birefringence. In the same way, the transition from SmA* to a non-helical SmC* phase (the helix being unwound by the sample surfaces or by an applied electric field) would be connected with a relatively high increase in Δn.

We have investigated the tilt-birefringence coupling in the case of standard FLC materials as well as several AFLC materials, and have noticed that the two classes generally exhibit quite different behaviour. In figure 7 (*a*) the SmA* texture of the short pitch FLC-mixture FLC 6430 (Hoechst) is compared with the texture in the SmC* phase. The sample is here on the verge of being surface-stabilized with the zero-field SmC* texture exhibiting helical as well as uniform unwound areas. The latter have essentially the same colour (first order cyan) as the SmA* texture. In other words, if the helix is removed from the SmC* phase the effective birefringence and thus the degree of orientational order is essentially the same in the two phases. In the helical areas, on the other hand, the birefringence is considerably reduced because of the averaging effect of the helical modulation, giving the first order reddish purple colour. Thus, the azimuthal biasing aspect of the director tilt seems to be less important in FLCs, suggesting that the orientational order in the SmA* phase of this materials class is relatively high.

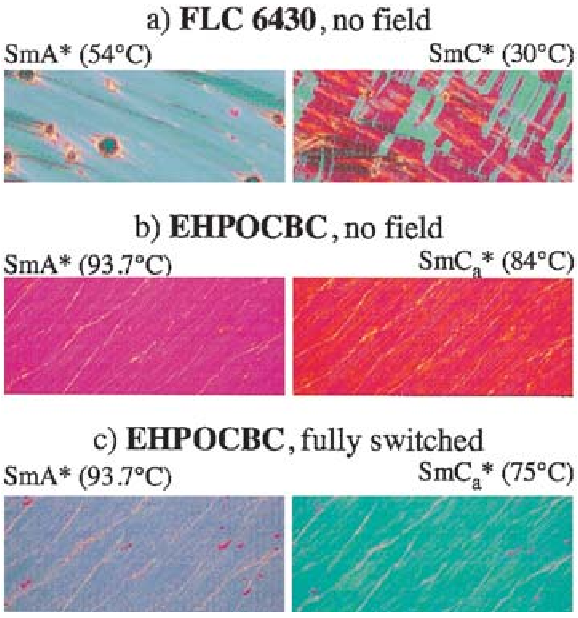

Figure 7. Textures of 4 μm thick samples of (*a*) FLC6430 in the SmA* (left) and SmC* (right) phases, (*b*) EHPOCBC in the SmA* (left) and SmC_a^* (right) phases, and (*c*) EHPOCBC under the influence of an electric field high enough for saturated switching, in the SmA* (left) and SmC_a^* (right) phases. The SmA*–SmC* transition of FLC6430 takes place at ~53°C, while the SmA*–SmC_a^* transition in EHPOCBC occurs at 92.7°C.

The case is quite different with the AFLC compound (*S*)-EHPOCBC, which has a direct SmA*–SmC_a^* transition. In figure 7 (*b*) we compare the zero-field SmA* texture with the corresponding texture in the SmC_a^* phase, and we see that the change in birefringence colour is quite small. EHPOCBC actually exhibits a helix inversion around 75°C, so the sample in the picture is partially surface-stabilized, resulting in pink (helical and anticlinic) and orange (non-helical, horizontal tilt plane, anticlinic) areas coexisting. The helicoidal domains have essentially the same birefringence colour as the SmA* phase, while the colour of the non-helical domains reflects a slightly lower birefringence. But considering that the director in SmA* is uniform, one should expect a distinct decrease in birefringence throughout the sample, particularly drastic in the non-helical areas, on cooling from SmA* to SmC_a^* if the degree of orientational order were similar in the two phases. The similarity in colour between the phases is therefore a clear indication that the orientational order is much lower in SmA* than in SmC_a^*, giving rise to an averaging of the optical properties almost equivalent to the local anticlinic structure and helical superstructure in the SmC_a^* phase.

In figure 7 (*c*) the effect of an applied electric field is shown in both phases. In the left figure we notice the increased birefringence as a result of the electroclinic effect in SmA* and in the right figure the considerably increased birefringence in the ferroelectric state of the SmC_a^* phase, i.e. in the state of much higher orientational (synclinic) order. It is noteworthy, that the birefringence colour is now actually close to that of the typical FLC sample in the absence of a helix, see figure 7 (*a*), suggesting that the orientational order in a synclinic state is essentially independent of material.

Although AFLCs exhibiting other chiral smectic C type phases between SmA* and SmC_a^* seem to have a slightly higher orientational order in the SmA* phase than EHPOCBC, a clear tilt–birefringence coupling is also generally seen there. On the other hand, all the compounds exhibiting direct SmA*–SmC_a^* transitions that we have studied showed the same behaviour as EHPOCBC, and we may thus in this sense classify such materials as typical 'de Vries type' smectics. This suggests that the anticlinic, antiferroelectric, SmC_a^* phase is particularly likely to form below a SmA* phase with very low orientational order. Most likely, this is related to the unusually large average molecular tilt already present in the SmA* phase of these materials, i.e. a very wide diffuse cone. Different materials in the chiral smectic C family may thus have SmA* phases of somewhat different character, illustrated at the one end by materials with a SmA*–SmC* transition (but no $\mathrm{SmC}_\mathrm{a}^*$ phase below) and at the other end by materials with a SmA*–$\mathrm{SmC}_\mathrm{a}^*$ transition.

It is now interesting to analyse our MHPOBC X-ray data in the light of the de Vries diffuse cone model. The general increase in layer spacing seen as the sample ages (see figure 6) indicates that either the molecules grow in size or the degree of orientational order increases, i.e. the diffuse cone gets narrower and taller [28–30]. The former explanation seems unlikely, as aggregation of molecules should lead to a much larger change than that observed. Hence, the X-ray data suggest that the orientational order increases as the sample ages, at least in the SmA* phase where the change in layer spacing is most pronounced. As argued above, this would fit well with the observation that the aged sample develops a SmC* phase, i.e. approaches the class of FLC materials.

4.4. *The role of spontaneous polarization*

In the case of chiral liquid crystals with a non-zero lateral molecular dipole, the appearance of director tilt is coupled with the spontaneous emergence of a uniform electric polarization $\mathbf{P}_\mathrm{s}$ within a layer. The magnitude of $\mathbf{P}_\mathrm{s}$ is proportional not only to the size of the molecular dipole, but also to the tilt angle θ. If the tilt is essentially in the same direction in neighbouring layers, as in the synclinic SmC* phase, an increasing tilt will produce a larger and larger electrostatic energy. In order to minimize this energy contribution, antiferroelectric liquid crystals, whose molecules always have large lateral dipoles, should therefore prefer an antipolar, hence anticlinic, structure. In this sense the anticlinic, antiferroelectric $\mathrm{SmC}_\mathrm{a}^*$ phase may appear to be the most natural polar tilted phase. Indeed, a few compounds are known, such as EHPOCBC, TFMHPOBC and 10BIMF6 (see the table) where the $\mathrm{SmC}_\mathrm{a}^*$ phase follows directly below the SmA* phase on cooling. However, the synclinic, synpolar SmC* phase is actually much more common in chiral smectics as a whole, and the direct SmA*–$\mathrm{SmC}_\mathrm{a}^*$ transition is quite rare. This shows that interactions promoting a synclinic structure, foremost interdigitation, are equally important.

The compensation of the polarization in the case of synclinic phases is obtained, on a larger scale than in $\mathrm{SmC}_\mathrm{a}^*$, by the helical superstructure. Only when $\mathbf{P}_\mathrm{s}$ reaches very high values will this be insufficient, and the anticlinic structure will be more stable. This is why synclinic phases generally appear when the director starts to tilt, while $\mathrm{SmC}_\mathrm{a}^*$ may appear as a low temperature phase when the tilt is sufficiently high. In the case that we have a direct SmA*–$\mathrm{SmC}_\mathrm{a}^*$ transition, the absence of a synclinic SmC* phase can, in this picture, be explained by the fact that the molecular tilt present in the SmA* phase is already too high, as suggested by the low orientational order observed in the SmA* phase of, for instance, EHPOCBC. We believe that the phase sequences of polar liquid crystals to a large extent are regulated by a complex interplay between the electrostatic interactions between permanent or induced dipoles, and steric interactions occurring across the layer boundaries, whereas the much weaker chiral interactions play a less dominant role.

Racemic mixtures of AFLC compounds constitute a special case. As pointed out by Fukuda and co-workers [33, 34], the polar pairing of unlike enantiomers (*R* and *S*) favours tilting in the same sense in adjacent layers, and hence synclinic order. In order to explain the preservation of the anticlinic structure in the racemate, they proposed that a spontaneous local optical resolution takes place, i.e. that molecules of the same enantiomeric nature group together (homochiral microdomains), an organization which increases the packing density. There are several well known cases of such a process occurring on crystallizing racemic mixtures of non-liquid crystalline organic compounds, allowing separation of the enantiomers in the solid state. The microscopic spontaneous polarization which could then be expected might be enough to stabilize the anticlinic phase, in particular as there is no helix present in a racemic mixture, which could otherwise take care of the polarization compensation. The stability is however much weaker than in an optically pure compound. If we lower the optical purity in a pure AFLC compound, thus lowering the magnitude of the spontaneous polarization, the SmC* (SmC for the racemate) phase develops even in compounds exhibiting a direct SmA*–$\mathrm{SmC}_\mathrm{a}^*$ transition in its pure form, as found by Isozaki *et al.* for the case of TFMHPOBC [35]. In fact, in the compound MHPBC (see the table), which in its optically pure form has the same phase sequence as that found for optically pure MHPOBC (i.e. no SmC* phase, but all three subphases above $\mathrm{SmC}_\mathrm{a}^*$), not only the subphases but even $\mathrm{SmC}_\mathrm{a}^*$ finally disappears on reducing the optical purity, such that in the racemate only SmA, SmC, and SmI_a are observed [35].

4.5. *On the origin of the subphases*

Our knowledge of the subphases is still very far from complete, but some basic facts are as follows. First, the subphases appear only in AFLCs. Such compounds generally have large lateral molecular dipoles, suggesting that polar interactions play an important role in stabilizing the subphase structures. Second, it is important to note that two of the subphases, SmC$^*_\gamma$ and SmC$^*_\beta$, appear below the SmC* phase when all five variants of the chiral smectic C family are present, while the third, SmC$^*_\alpha$, appears between the SmC* and SmA* phase in these cases. In other words, the SmC$^*_\alpha$ phase is the highest temperature chiral smectic C type phase and thus stands out from the other subphases as apparently having higher symmetry than SmC*, whereas SmC$^*_\gamma$ and SmC$^*_\beta$ have lower symmetry.

Another important difference between the subphases is that there are no examples of a direct transition SmA*–SmC$^*_\beta$ or SmA*–SmC$^*_\gamma$, while the direct SmA*–SmC$^*_\alpha$ transition (usually mainly second order) is frequent among optically pure AFLC compounds. This may be explained in terms of polar interactions: if $\mathbf{P}_s$ is very small, as it is directly below the second order onset of tilt, we would expect only the helical modulation caused by the chiral interaction, as in SmC$^*_\alpha$ or SmC*. At higher $\mathbf{P}_s$ values, the free energy will eventually be further reduced by introducing an additional polarization cancellation on a smaller scale, leading to the partial or full polarization compensation on the unit cell level characteristic of the SmC$^*_\beta$, SmC$^*_\gamma$ and SmC$^*_a$ phases. The role of $\mathbf{P}_s$ is also supported by an experiment performed by Isozaki *et al.* [20] where the SmC$^*_\alpha$ phase turned out to be present, as the only subphase, in a polarization–compensated (but not helix–compensated) mixture of (*R*)-MHPBC and (*S*)-TFMHPBC. The other two subphases, only present in MHPBC, disappeared even at very small quantities of TFMHPBC in the mixture. The bunching together of SmC$^*_\alpha$, SmC$^*_\beta$ and SmC$^*_\gamma$ into the collective concept 'subphases' is thus somewhat unfortunate, as it is clear that the first of these phases must be discussed separately from the two latter.

The proposed distorted clock SmC$^*_\beta$ and SmC$^*_\gamma$ structures are interesting in the sense that they actually have two superposed helical structures. In addition to the large scale, 'optical', helical superstructure (period 1–5 μm) present also in SmC* and SmC$^*_a$, these two subphases are already twisted on the unit cell level, with a period of four and three layers, respectively. Consequently, the unit cell must also have a certain handedness, or twisting sense. Cady *et al.* reported that the unit cell twisting sense of the SmC$^*_\beta$ phase of one compound (MHDDOPTCOB) was the same as that of the large scale helix [15]. At first sight it might seem natural that this should always be so, at least if the two different helices have a common origin, but this cannot always be the case. If it were, the very common event of a helix inversion within a subphase [36–38] or at its border [17] would imply a rather drastic change in unit cell structure over a very small temperature range. The unit cell would have to go from a distorted clock of one handedness, via an in-plane flat structure, to a distorted clock of the opposite handedness. However, the two different helices actually have no inherent coupling, as illustrated in figure 8 for the case of the SmC$^*_\gamma$ phase (the SmC$^*_\beta$ case is completely analogous). This figure schematically shows the cases of left- and right-handed macroscopic helices superimposed onto the same right-handed unit cell. It is obvious that a change of handedness of the macroscopic helix requires only a minor structural change, essentially not affecting the unit cell structure. It is an interesting challenge for future work on the SmC$^*_\beta$ and SmC$^*_\gamma$ phases to elucidate the origin of the unit cell twist and investigate whether one can find a relation between the unit cell handedness and the molecular structure.

4.6. *On the subphase terminology*

The new understanding of the MHPOBC phase sequence has paved a way for a solution to the terminology problem which has been an inherent characteristic of AFLC research almost since the start. The confusing and misleading notations 'AF' and 'SmC$^*_{\mathrm{FI2}}$', which have up to now often been used to designate the antiferroelectric subphase, can now be replaced with SmC$^*_\beta$. In

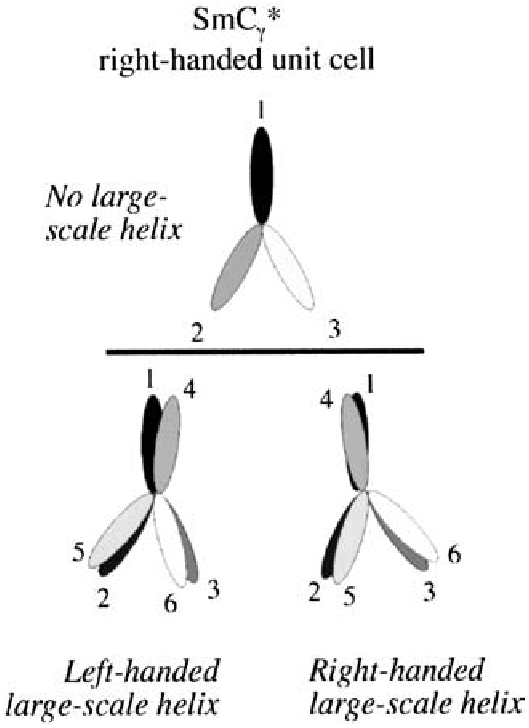

Figure 8. An illustration of how the macroscopic helical superstructure can change from left- to right-handed without affecting the handedness of the SmC$^*_\gamma$ unit cell twist, which here is drawn right-handed. The layer numbering goes from the paper plane to the reader, i.e. layer 1 is the farthest away, layer 6 is the closest. The situation for the SmC$^*_\beta$ phase is analogous.

general, we strongly advocate ending the use of terms indicating physical *properties*, as this habit invariably leads to incorrect statements. (For instance, the subscript 'FI2' stands for '*Ferri*electric', but the phase in question has long been known to be antiferroelectric.) The question of the physical properties of a certain structure is complicated in itself and ought to be a secondary consideration, especially as it requires knowledge of the structure in its greatest detail. There are many indications that such details of the subphase structures may vary between different compounds or with temperature (e.g. distorted clock with varying distortion angles), hence specific physical properties like ferro-, or ferrielectric could not even be attributed to the repeating units as such. We find that the simplest and most natural choice for the terminology is a return to the original scheme proposed by the Fukuda school, a scheme which is logical and free from insinuations of any particular properties for any of the subphases. Following this line, we suggest that also the notation $\mathrm{SmC}^*_{\mathrm{FI1}}$ for the SmC^*_{γ} phase be abolished. The scientific discussion on antiferroelectric liquid crystals has much to gain from a single, consistent and logical terminology.

5. Conclusions

We have shown that the antiferroelectric liquid crystal MHPOBC, which in its optically pure state exhibits the three subphases SmC^*_{α}, SmC^*_{β} and SmC^*_{γ}, but no SmC* phase, is chemically degraded under normal experimental conditions, such that the SmC* phase appears and eventually replaces the SmC^*_{β} phase. Even in thick cells, where subphases are generally less influenced by the surfaces, the degradation can be rapid enough to change the phase sequence considerably during the course of an experiment. X-ray experiments suggest that the change is connected to an increase in orientational order and increased layer interdigitation, corresponding to a reduction in the translational order. We believe that a high degree of translational order, just like a high value of tilt and spontaneous polarization, is an essential property of antiferroelectric liquid crystals. At high tilt, the anticlinic order reduces the permeation of molecules from layer to layer such that the smectic layer itself becomes more well defined. Inversely, if we lower the smectic order, permeation increases and we increase the orientational order, because the orientational freedom of a certain molecule is reduced through steric hindrance by neighbours not only in the same layer, but also in the layers above and below. Thus, a reduction in translational order tends to diminish the tilt (and polar interactions), destabilizing the anticlinic structure and instead promoting a synclinic phase. As many AFLC materials have a very high degree of disorder in the molecular tilting direction in the SmA* phase, the diffuse cone model of de Vries seems particularly adequate for such materials.

The suppression of the subphases and the emergence of SmC* when an AFLC compound is mixed with chemically or enantiomerically different molecules, may thus be understood as arising mainly from the increased molecular interdigitation across the layer boundaries and from the reduced tilt, hence effective $\mathbf{P}_s$, in connection with it. Chiral interactions are certainly responsible, together with the polar interactions, for the distorted helical unit cells found in SmC^*_{β} and SmC^*_{γ}, which have a certain handedness; but we find it unlikely that the suppression of subphases should be related solely to a decrease in the strength of chiral interactions. It is interesting to note that the large scale helical superstructure in SmC^*_{β} and SmC^*_{γ} can easily change handedness, by a minor structural distortion, without changing the handedness of the unit cell itself.

We would like to thank the groups of professor R. Dabrowski (Warszaw, Poland), for supplying the exceptionally pure sample of (*S*)-MHPOBC, and of professor G. Heppke (Berlin, Germany), for the sample of (*S*)-EHPOCBC. We also thank J. Ivens for her assistance in the X-ray measurements. Financial support from the German Academic Exchange Agency (DAAD), the Chalmers School of Materials Science, and the Swedish Foundation for Strategic Research is gratefully acknowledged.

References

[1] Chandani, A. D. L., Ouchi, Y., Takezoe, H., and Fukuda, A., 1989, *Jpn. J. appl. Phys. Lett.*, **28,** L1261.

[2] Fukui, M., Orihara, H., Yamada, Y., Yamamoto, N., and Ishibashi, Y., 1989, *Jpn. J. appl. Phys. Lett.*, **28,** L849.

[3] Hiraoka, K., Taguchi, A., Ouchi, Y., Takezoe, H., and Fukuda, A., 1990, *Jpn. J. appl. Phys. Lett.*, **29,** L103.

[4] Li, J.-F., Shack, E. A., Yu, Y.-K., Wang, X.-Y., Rosenblatt, C., Neubert, M. E., Keast, S. S., and Gleeson, H., 1996, *Jpn. J. appl. Phys. Lett.*, **35,** L1608.

[5] Sako, T., Kimura, Y., Hayakawa, R., Okabe, N., and Suzuki, Y., 1996, *Jpn. J. appl. Phys. Lett.*, **35,** L114.

[6] Jakli, A., 1999, *J. appl. Phys.*, **85,** 1101.

[7] Tatemori, S., Uehara, H., Hatano, J., Saito, S., Saito, H., and Okabe, E., 1999, in Proceedings from FLC'99, August 29–September 3 1999; Darmstadt, Germany 2000, *Ferroelectrics*, **244,** 241.

[8] Gorecka, E., Pociecha, D., Cepic, M., Zeks, B., and Dabrowski, R., 2002, *Phys. Rev. E*, **65,** 061703-1.

[9] Okabe, N., Suzuki, Y., Kawamura, I., Isozaki, T., Takezoe, H., and Fukuda, A., 1992, *Jpn. J. appl. Phys. Lett.*, **31,** L793.

[10] Panarin, Y. P., Kalinovskaya, O., and Vij, J. K., 1998, *Liq. Cryst.*, **25,** 241.

[11] Rudquist, P., Kruerke, D., Lagerwall, S. T., MacLennan, J. E., Clark, N. A., and Walba, D. M., 1999, in Proceedings from FLC'99, August 29–September 3 1999; Darmstadt, Germany 2000, *Ferroelectrics*, **246,** 927.

[12] Mach, P., Pindak, R., Levelut, A. M., Barois, P., Nguyen, H. T., Huang, C. C., and Furenlid, L., 1998, *Phys. Rev. Lett.*, **81,** 1015.

[13] Mach, P., Pindak, R., Levelut, A. M., Barois, P., Nguyen, H. T., Baltes, H., Hird, M., Toyne, K., Seed, A., Goodby, J. W., Huang, C. C., and Furenlid, L., 1999, *Phys. Rev. E*, **60,** 6793.

[14] Johnson, P. M., Olson, D. A., Pankratz, S., Nguyen, H. T., Goodby, J. W., Hird, M., and Huang, C. C., 2000, *Phys. Rev. Lett.*, **84,** 4870.

[15] Cady, A., Pitney, J. A., Pindak, R., Matkin, L. S., Watson, S. J., Gleeson, H. F., Cluzeau, P., Barois, P., Levelut, A. M., Caliebe, W., Goodby, J., Hird, M., and Huang, C. C., 2001, *Phys. Rev. E*, **64,** 050702/1.

[16] Akizuki, T., Miyachi, K., Takanishi, Y., Ishikawa, K., Takezoe, H., and Fukuda, A., 1999, *Jpn. J. appl. Phys.*, **38,** 4832.

[17] Lagerwall, J. P. F., Parghi, D. D., Krüerke, D., Gouda, F., and Jägemalm, P., 2002, *Liq. Cryst.*, **29,** 163.

[18] Rosenblatt, C. S., Pindak, R., Clark, N. A., and Meyer, R. B., 1977, *J. Phys.*, **38,** 1105.

[19] Cepic, M., and Zeks, B., 2001, *Phys. Rev. Lett.*, **87,** 085501/1.

[20] Isozaki, T., Ishikawa, K., Takezoe, H., and Fukuda, A., 1993, in Proceedings from FLC'93, September 28–October 1 1993, Tokyo, Japan; 1993, *Ferroelectrics*, **147,** 121.

[21] Isozaki, T., Fujikawa, T., Takezoe, H., Fukuda, A., Hagiwara, T., Suzuki, Y., and Kawamura, I., 1993, *Phys. Rev. B*, **48,** 13 439.

[22] Wu, S. L., Hsieh, W. J., and Yu, M. C., 2000, Poster 27E-38P at ILCC'2000, July 2000, Sendai, Japan.

[23] Als-Nielsen, J., Birgeneau, R. J., Kaplan, M., Litster, J. D., and Safinya, C. R., 1977, *Phys. Rev. Lett.*, **39,** 352.

[24] Takanishi, Y., Ikeda, A., Takezoe, H., and Fukuda, A., 1995, *Phys. Rev. E*, **51,** 400.

[25] Jin, B., Zhihua, L., Takanishi, Y., Ishikawa, K., Takezoe, H., Fukuda, A., Kakimoto, M., and Kitazume, T., 1996, *Phys. Rev. E*, **53,** R4295.

[26] Nishiyama, I., and Goodby, J. W., 1992, *J. mater. Chem.*, **2,** 1015.

[27] Booth, C. J., Dunmur, D. A., Goodby, J. W., Haley, J., and Toyne, K. J., 1996, *Liq. Cryst.*, **20,** 387.

[28] De Vries, A., Ekachai, A., and Spielberg, N., 1979, *Mol. Cryst. liq. Cryst. Lett.*, **49,** 143.

[29] De Vries, A., 1979, *Mol. Cryst. liq. Cryst. Lett.*, **49,** 179.

[30] De Vries, A., 1979, *J. chem. Phys.*, **71,** 25.

[31] Rieker, T. P., Clark, N. A., Smith, G. S., Parmar, D. S., Sirota, E. B., and Safinya, C. R., 1987, *Phys. Rev. Lett.*, **59,** 2658.

[32] Selinger, J. V., Collings, P. J., and Shashidhar, R., 2001, *Phys. Rev. E*, **64,** 061705/1.

[33] Takanishi, Y., Hiraoka, K., Agrawal, V. K., Takezoe, H., Fukuda, A., and Matsushita, M., 1991, *Jpn. J. appl. Phys.*, **30,** 2023.

[34] Fukuda, A., Takanishi, Y., Isozaki, T., Ishikawa, K., and Takezoe, H., 1994, *J. mater. Chem.*, **4,** 997.

[35] Isozaki, T., Takezoe, H., Fukuda, A., Suzuki, Y., and Kawamura, I., 1994, *J. mater. Chem.*, **4,** 237.

[36] Gorecka, E., 2001, personal communication.

[37] Gisse, P., Lorman, V. L., Pavel, J., and Nguyen, H. T., 1995, in Proceedings of FLC'95, July 23–27 1995, Cambridge, UK; 1996, *Ferroelectrics*, **178,** 297.

[38] Gisse, P., Sidir, M., Lorman, V. L., Farhi, R., Pavel, J., and Nguyen, H. T., 1997, *J. Phys. II Fr.*, **7,** 1817.

[39] Olson, D. A., Pankratz, S., Johnson, P. M., Cady, A., Nguyen, H. T., and Huang, C. C., 2001, *Phys. Rev. E*, **63,** 061711/1.

[40] Heppke, G., Lötzsch, D., Bömelburg, J., and Rauch, S., 1998, *Mol. Cryst. liq. Cryst.*, **317,** 65.

[41] Yamada, Y., Mori, K., Yamamoto, N., Hayashi, H., Nakamura, K., and Yamawaki, M., 1989, *Jpn. J. appl. Phys. Lett.*, **28,** L1606.